

# A General Approach for Transferring Hydrophobic Nanocrystals into Water

Tierui Zhang, Jianping Ge, Yongxing Hu, and Yadong Yin\*

*Department of Chemistry, University of California, Riverside, California 92521*

*Received August 5, 2007; Revised Manuscript Received August 29, 2007*

## ABSTRACT

Hydrophobic inorganic nanocrystals have been transferred from organic solvent to aqueous solution through a robust and general ligand exchange procedure. Polyelectrolytes such as poly(acrylic acid) and poly(allylamine) are used to replace the original hydrophobic ligands on the surface of nanocrystals at an elevated temperature in a glycol solvent and eventually render the nanocrystals highly water soluble. The physical properties of the nanocrystals, such as superparamagnetism, photocatalytic activity, and photoluminescence, are maintained or improved after ligand exchange.

Impressive progress has been made in synthesis of colloidal nanocrystals with well-defined structures.<sup>1–4</sup> Among known chemical routes, high-temperature thermolysis of organo-metallic species in nonpolar solvents has been widely shown to be a general approach capable of producing colloidal nanostructures with narrow size distribution, low crystalline defects, and tunable shapes. Despite its success in synthesizing a wide variety of compositions, this approach typically produces nanocrystals with hydrophobic surfaces. The resulting insolubility of the nanocrystals in water greatly limits their applications in important fields such as drug delivery, biodetection, biolabeling, and catalysis in aqueous solution. To this end, several strategies have been developed to transfer nanocrystals with hydrophobic surfaces into water. One popular method is based on ligand exchange, where the hydrophobic surfactants on the particle surfaces are replaced by small molecules containing polar groups on both ends.<sup>5–9</sup> Because the exchange is usually performed at room temperature and the exchange ratio is typically low, irreversible desorption of new surfactants from the particle surface may sometimes occur, eventually destabilizing the system and resulting in aggregation. Alternatively, the nanocrystals can be transferred into water through micelle-like interactions between the hydrophobic surface ligands and an amphiphilic polymer or lipids.<sup>10–13</sup> This method has the advantage of being general to a large number of materials, but the subsequent surface modification is usually complicated due to the dynamic nature of the outer layer coating. Pellegrino et al. have been able to stabilize the amphiphilic polymer layer through crosslinking, making it convenient for further chemical processing.<sup>11</sup>

In this paper, we describe a robust ligand exchange method that uses short-chain hydrophilic polyelectrolyte molecules to replace the original hydrophobic ligands at an elevated temperature in a glycol solvent. Figure 1 schematically illustrates the general principle of our approach. The polyelectrolyte molecules are chosen on the basis of strong coordination of their functional groups to the nanocrystal surface, with typical examples including poly(acrylic acid) (PAA), poly(allylamine) (PAAm), and poly(sodium styrene sulfonate) (PSS). Diethylene glycol (DEG) was selected as the polar solvent because of its high boiling point (~245 °C), high dissolving capacity for polyelectrolytes, and high miscibility with both water and typical organic solvents. Similar compounds such as ethylene glycol and triethylene glycol can also be used for this purpose. In a typical process, a toluene solution containing hydrophobic nanocrystals is rapidly injected into a heated mixture of DEG and exchanging ligands. The solution becomes turbid immediately because of the insolubility of hydrophobic nanocrystals in the polar solvent. Upon continued heating at a higher temperature close to the boiling point of the solvent, the solution slowly turns clear, indicating the occurrence of ligand exchange and dissolution of nanocrystals in DEG. The nanocrystals can then be precipitated, for example, by adding excess amount of diluted aqueous solution of hydrochloric acid and finally redispersed in water by transforming remaining uncoordinated groups into ionized form.

Compared to previously reported ligand exchange processes, our approach has several advantages. First, the exchange reaction is performed at relatively high temperatures so that the dynamic solvation of the ligands favors the exchange of original surfactants with new ones through mass action. Second, each polyelectrolyte chain binds to the nanocrystal surface through multiple anchoring points, providing more robust surface adhesion than that achievable

\* To whom correspondence should be addressed. E-mail: yadong.yin@ucr.edu.

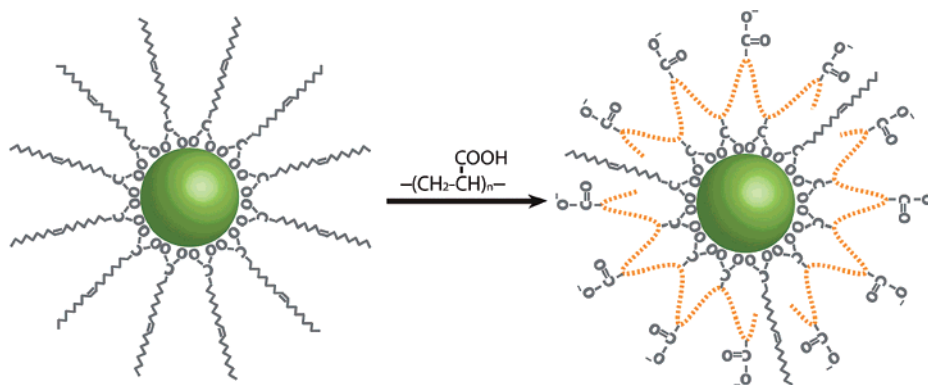


**Figure 1.** Schematic illustration of the general principle of the ligand exchange approach by using oleic acid coated iron oxide nanocrystals as a model system. Ligand exchange with PAA in a polyol solvent such as DEG at high temperature makes these nanocrystals water soluble.

with a small molecule that typically has only one binding group.<sup>14</sup> The strong binding also prevents desorption of ligands from the particle surface, which has been one of the sources of toxicity in practical applications. Third, the abundant uncoordinated groups on each polymer chain extend into water, making the particles highly soluble. In addition, these remaining functional groups such as  $-\text{COOH}$  and  $-\text{NH}_2$  are available for further surface modification, for example, by coupling to bioactive molecules. Fourth, the reductive environment provided by the glycol solvent at high temperature allows processing of materials liable to oxidation, as demonstrated later in the example of CdSe. Fifth, the process described here uses commercial polyelectrolyte materials, which are much more economical than some surfactants such as phospholipids or specially synthesized polymers used in other procedures.<sup>15</sup>

We first demonstrate the feasibility of this method by transferring hydrophobic iron oxide nanocrystals to water. Iron oxide nanocrystals, typically superparamagnetic, hold great promise in many important applications including ferrofluids, medical imaging, and targeted drug delivery.<sup>16–19</sup> In contrast to the room-temperature precipitation method, which produces nanoparticles with broad size distributions, high-temperature thermolysis routes have recently been very successful in producing highly monodisperse iron oxide nanocrystals in nonpolar solvents.<sup>2,20–23</sup> It is therefore of great importance to find an effective approach to make these nanocrystals soluble in water.<sup>13,24,25</sup>

Superparamagnetic  $\gamma\text{-Fe}_2\text{O}_3$  nanocrystals capped with oleic acid were first synthesized using a thermolysis process reported previously.<sup>22</sup> As shown in the transmission electron microscopy image (TEM) in Figure 2a, these nanocrystals are spherical, narrow in size distribution, and have an average diameter of  $\sim 11$  nm. Short-chain PAA with  $\sim 25$  repeating units is used as the exchanging ligand because of the strong coordination of carboxylates to iron oxide surface. Figure 2b shows a typical TEM image of the nanocrystals after ligand exchange. They remain monodisperse in size without obvious shape change and aggregation. Similar to the original nanocrystals in toluene, a concentrated solution of nanocrystals in water shows ferrofluidic behavior when subjected to an external magnetic field (Figure 2c). No obvious

precipitation can be found even after exposure of the solution to a magnetic field over 5 min, demonstrating a stable dispersion of the nanocrystals in water. The solution returns to normal conditions when the external magnetic field is removed, displaying the expected superparamagnetic behavior. In addition, the aqueous solution of  $\gamma\text{-Fe}_2\text{O}_3$  nanocrystals remains very stable when the pH value is above 5.<sup>26–28</sup> No obvious change was found after storing the sample for more than 3 months under ambient conditions. We have also examined the thermal stability of the dispersion by refluxing the aqueous solution for 1 day, which remained essentially the same without noticeable precipitation or loss of superparamagnetic property.

Fourier transform infrared (FT-IR) spectroscopy was used to characterize the functional groups present on the surface of nanocrystals after the ligand exchange. In Figure 3a (top), the weak stretching mode of the  $-\text{COOH}$  group at  $1709\text{ cm}^{-1}$  suggests the presence of trace amounts of free oleic acid on the surface of nanocrystals before ligand exchange. This band is significantly enhanced and shifted to  $1732\text{ cm}^{-1}$  after ligand exchange by PAA, suggesting an increase in the quantity of the  $-\text{COOH}$  groups on the particle surface.<sup>29</sup> The bands at  $1522$  and  $1427\text{ cm}^{-1}$  for the original sample can be assigned to the antisymmetric and symmetric vibration modes of the  $-\text{COO}^-$  group, indicating the adsorption of oleic acid on the nanocrystal surface through the bidentate bonds.<sup>14</sup> After ligand exchange, a new band related to the symmetric vibration modes of the  $-\text{COO}^-$  group appears at  $1396\text{ cm}^{-1}$ . Additionally, the shoulder at  $2955\text{ cm}^{-1}$  associated with the asymmetrical stretching mode of  $-\text{CH}_3$  groups became inconspicuous after ligand exchange. On the basis of these observations, one can conclude that PAA bonds to the nanocrystal surface in place of oleic acid although FT-IR cannot provide quantitative information on the amount of PAA on the particle surface.

Thermogravimetric analysis (TGA) measurements were conducted in order to determine the ligand exchange efficiency. As shown in Figure 3b (top), the major weight loss of  $\sim 9.3\%$  spans from  $\sim 200$  to  $550^\circ\text{C}$  due to the desorption of oleic acid, in agreement with the report in literature.<sup>30</sup> After ligand exchange, the initial mass loss of physically adsorbed water increases from  $\sim 0.66\%$  in the original sample

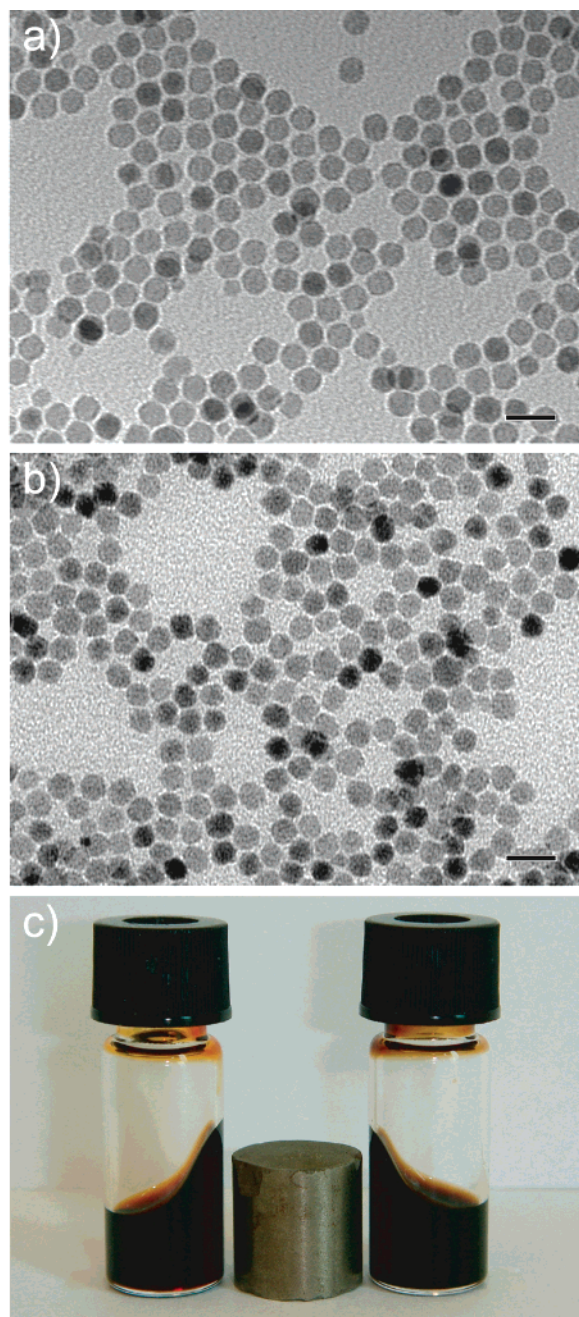


**Figure 2.** TEM images of  $\gamma$ -Fe<sub>2</sub>O<sub>3</sub> nanocrystals (a) before and (b) after ligand exchange. Scale bars are 20 nm. (c) Photographs showing the ferrofluidic behavior of  $\gamma$ -Fe<sub>2</sub>O<sub>3</sub> nanocrystals in toluene (left) and water (right) in the presence of an external magnet (middle).

to  $\sim 1.0\%$ , due probably to the hydrophilic nature of PAA capped  $\gamma$ -Fe<sub>2</sub>O<sub>3</sub> nanocrystals (Figure 3b (bottom)). The major mass loss of  $\sim 13.8\%$  ranging from  $\sim 200$  to  $550$  °C can be ascribed to the decomposition of PAA and oleic acid.<sup>31</sup> Because the decomposition of both surfactants occurs at a similar temperature range, we can only estimate the weight ratio of surface PAA to Fe<sub>2</sub>O<sub>3</sub> between 5.9% (in the extreme case where no oleic acid has been removed) and 16.2% (in another extreme case where oleic acid has been completely replaced). With an average particle size of 11 nm and the density of iron oxide of  $5.24 \text{ g cm}^{-3}$ , we can further estimate the number of PAA chains attached to the surface of each

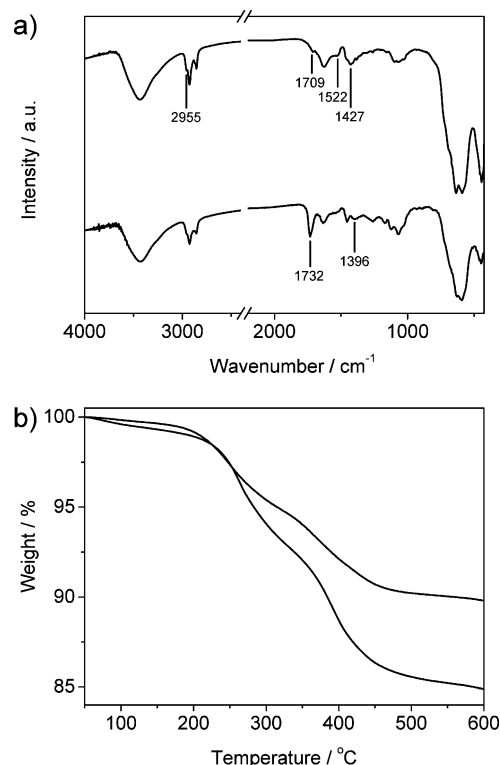


**Figure 3.** (a) FT-IR spectra of  $\gamma$ -Fe<sub>2</sub>O<sub>3</sub> nanocrystals before (top) and after (bottom) ligand exchange using PAA. (b) TGA curves of  $\gamma$ -Fe<sub>2</sub>O<sub>3</sub> nanocrystals before (top) and after (bottom) ligand exchange. The measurements were performed under N<sub>2</sub> atmosphere.

$\gamma$ -Fe<sub>2</sub>O<sub>3</sub> nanocrystal ranging from  $\sim 72$  to 198. Additionally, the mass losses are consistent between batches, indicating the good reproducibility of surface coverage.

The ligand exchange route using hydrophilic PAA to replace hydrophobic surfactants is general for oxide nanocrystals. Here, we further demonstrate its feasibility with titania (TiO<sub>2</sub>), an important semiconductor material for its wide applications, chemical stability, and nontoxicity. In particular, TiO<sub>2</sub> is one of the most widely used photocatalysts for applications in an aqueous environment such as water splitting.<sup>32</sup> Reduction of the particle size to the nanometer scale is desirable as it yields significantly increased surface area.<sup>33,34</sup> However, it has been extremely difficult to synthesize well-defined TiO<sub>2</sub> nanocrystals directly soluble in water.<sup>35,36</sup> Again, thermolysis in nonpolar solvent has been able to produce samples with increased uniformity, high crystallinity, and controlled morphologies, although there is still some room for improving the monodispersity.<sup>37–39</sup>

We synthesized TOPO capped anatase nanocrystals with a slightly elongated shape and an average diameter of  $\sim 6.0$  nm using a method reported in literature (Figure 4a).<sup>37</sup> Ligand exchange with PAA at  $240$  °C for 5 min in DEG leads to the formation of a transparent solution. Polyelectrolytes containing sulfonate groups such as PSS can also be used for the same purpose under similar reaction conditions. TEM measurement confirms that the products still maintain the original size and shape (Figure 4b). More importantly, this ligand exchange procedure is also general to nanocrystals with other shapes such as hydrophobic TiO<sub>2</sub>



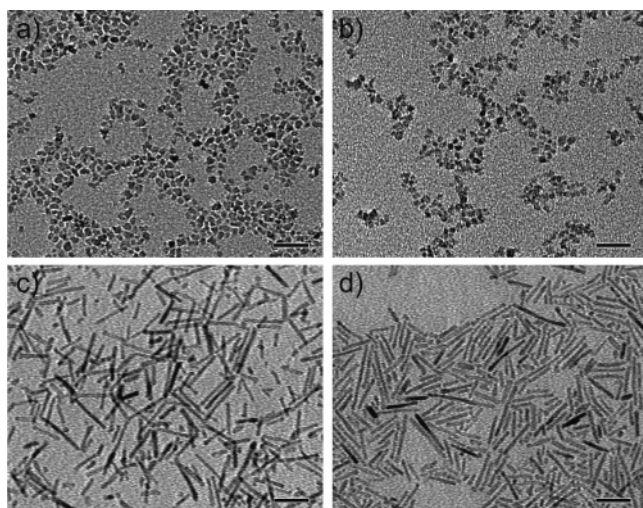


**Figure 4.** TEM images of TiO<sub>2</sub> nanodots (a) before and (b) after ligand exchange, and TiO<sub>2</sub> nanorods (c) before and (d) after ligand exchange. Scale bars are 30 nm.

nanorods capped with oleic acid.<sup>34</sup> In this case, the system took much longer ( $\sim 6$  h) to become transparent. As displayed in Figure 4d, the recovered nanorods show essentially no change in morphology except the much higher percentage of long rods. The enrichment of long rods is a result of unintentional size selection during multiple washing steps.

The water-soluble TiO<sub>2</sub> nanocrystals can be readily used for photocatalytic applications. We have performed a simple demonstration of using these nanocrystals for photodegradation of rhodamine 6G (R6G), a common dye pollutant and also a typical probe for photoactivity tests.<sup>40,41</sup> R6G was decomposed by 54.8% and 94.4% without and with photocatalyst of TiO<sub>2</sub> nanocrystals after 30 min UV irradiation, respectively, demonstrating their potential use as water-soluble photoactive materials (Supporting Information).

The polyelectrolyte surfactant for a particular system is selected based on the strength of adhesion of its metal-coordinating groups to the nanocrystals. For example, PAA works for most metal oxides, but it cannot effectively exchange TOPO on CdSe nanocrystal surface. Fortunately, a number of other polyelectrolytes containing different functional groups can be used for the purpose of ligand exchange. In the case of CdSe, for example, PAAm can effectively replace TOPO if heated with the nanocrystals in DEG at an elevated temperature and finally stabilize the nanocrystal in water. This is because of the strong coordination power of primary amines to the surface atoms on various metals, metal oxides, and chalcogenides.<sup>2,42</sup> As shown in Figure 5a and b, monodisperse nanocrystals of CdSe of  $\sim 6$  nm in diameter can be successfully transferred to water. The nanocrystals appear slightly different from the original sample, probably due to the lower contrast when the particles are coated with a relatively thick layer of polymer.<sup>11</sup> As shown in Figure 5c, fluorescence emission peaks for the samples before and after ligand exchange are both located at 628 nm, indicating no obvious change in the particle size. The emission peak for the sample in water broadens asymmetrically by about 4 nm (fwhm) toward shorter

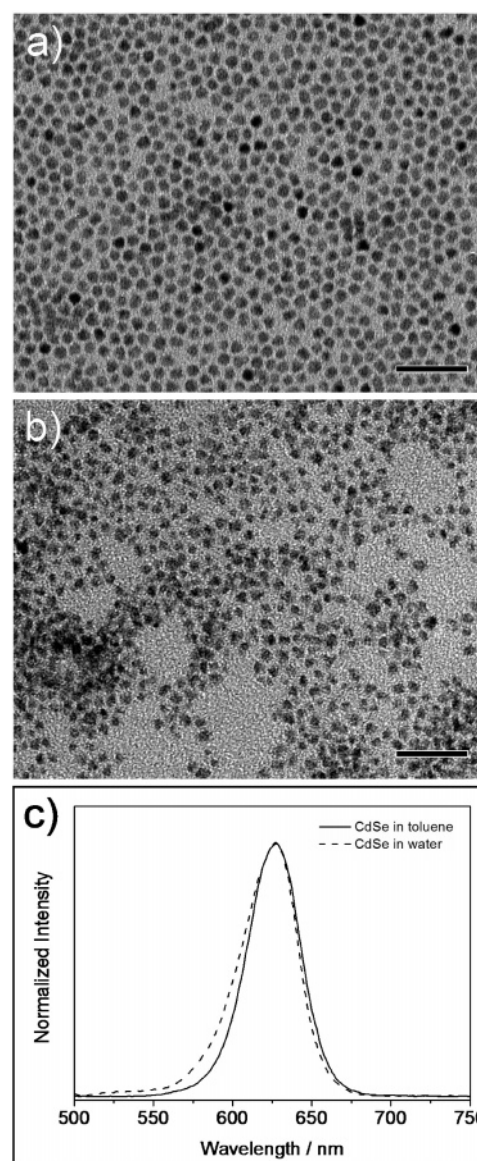


**Figure 5.** TEM images of CdSe nanocrystals (a) before and (b) after ligand exchange. Scale bars are 40 nm. (c) Fluorescence spectra of hydrophobic CdSe nanocrystals capped with TOPO in toluene (solid line) and hydrophilic nanocrystals capped with PAAm in water (dash line). The excitation wavelength is 480 nm.

wavelengths in comparison to that of the original sample. Additionally, the water-soluble CdSe nanocrystals show  $\sim 54\%$  higher quantum yield than the sample without ligand exchange. Both the increased fwhm and the enhanced quantum yield are consistent with a surface-state change of CdSe nanocrystals due to the replacement of TOPO with PAAm. Amine groups are well known to effectively passivate surface traps participating in nonradioactive recombination processes, thus improving the photoluminescence efficiency of CdSe nanocrystals.<sup>43,44</sup>

In summary, a unique and general approach has been developed to successfully transfer hydrophobic inorganic nanocrystals such as  $\gamma$ -Fe<sub>2</sub>O<sub>3</sub>, TiO<sub>2</sub>, and CdSe into water through a robust ligand exchange procedure. This is made possible by use of polyelectrolytes with multiple and strong binding groups and by the thermal energy available for

effective ligand exchange provided by the high reaction temperature in the polar solvent DEG. The resulted aqueous dispersions of nanocrystals remain stable over months without obvious precipitation/aggregation. This approach may represent an important step toward the missing link between various high-quality hydrophobic nanocrystals produced by thermolysis methods and their important biomedical and photocatalytic applications in which water solubility is a prerequisite.

**Acknowledgment.** Y. Yin thanks the University of California, Riverside for start-up funds and the Regent's Faculty fellowship. We thank Prof. Y. Yan, Z. Chen, and M. Sun for assistance with TGA measurement and Dr. K. N. Bozhilov and S. McDaniel at the Central Facility for Advanced Microscopy and Microanalysis at UCR for assistance with TEM measurements.

**Supporting Information Available:** Experimental procedures, photocatalytic measurements of TiO<sub>2</sub> nanocrystals. This material is available free of charge via the Internet at <http://pubs.acs.org>.

## References

- Yin, Y.; Alivisatos, A. P. *Nature* **2005**, *437*, 664–670.
- Park, J.; Joo, J.; Kwon, S. G.; Jang, Y.; Hyeon, T. *Angew. Chem., Int. Ed.* **2007**, *46*, 4630–4660.
- Wang, X.; Zhuang, J.; Peng, Q.; Li, Y. *Nature* **2005**, *437*, 121–124.
- Wiley, B.; Sun, Y.; Chen, J.; Cang, H.; Li, Z.-Y.; Li, X.; Xia, Y. *MRS Bull.* **2005**, *30*, 356–361.
- Chan, W. C. W.; Nie, S. M. *Science* **1998**, *281*, 2016–2018.
- Kim, M.; Chen, Y.; Liu, Y.; Peng, X. *Adv. Mater.* **2005**, *17*, 1429–1432.
- De Palma, R.; Peeters, S.; Van Bael, M. J.; Van den Rul, H.; Bonroy, K.; Laureyn, W.; Mullens, J.; Borghs, G.; Maes, G. *Chem. Mater.* **2007**, *19*, 1821–1831.
- Kim, S.; Bawendi, M. G. *J. Am. Chem. Soc.* **2003**, *125*, 14652–14653.
- Dubois, F.; Mahler, B.; Dubertret, B.; Doris, E.; Mioskowski, C. *J. Am. Chem. Soc.* **2007**, *129*, 482–483.
- Fan, H.; Yang, K.; Boye, D. M.; Sigmon, T.; Malloy, K. J.; Xu, H.; Lopez, G. P.; Brinker, C. J. *Science* **2004**, *304*, 567–571.
- Pellegrino, T.; Manna, L.; Kudera, S.; Liedl, T.; Koktysh, D.; Rogach, A. L.; Keller, S.; Radler, J.; Natile, G.; Parak, W. J. *Nano Lett.* **2004**, *4*, 703–707.
- Yu, W. W.; Chang, E.; Falkner, J. C.; Zhang, J.; Al-Somali, A. M.; Sayes, C. M.; Johns, J.; Drezek, R.; Colvin, V. L. *J. Am. Chem. Soc.* **2007**, *129*, 2871–2879.
- Wang, Y.; Wong, J. F.; Teng, X.; Lin, X. Z.; Yang, H. *Nano Lett.* **2003**, *3*, 1555–1559.
- Willis, A. L.; Turro, N. J.; O'Brien, S. *Chem. Mater.* **2005**, *17*, 5970–5975.
- Nikolic, M. S.; Krack, M.; Aleksandrovic, V.; Kornowski, A.; Forster, S.; Weller, H. *Angew. Chem., Int. Ed.* **2006**, *45*, 6577–6580.
- Weissleder, R.; Cheng, H. C.; Bogdanova, A.; Bogdanov, A. *J. Magn. Reson. Imaging* **1997**, *7*, 258–263.
- Petri-Fink, A.; Chastellain, M.; Juillerat-Jeanneret, L.; Ferrari, A.; Hofmann, H. *Biomaterials* **2005**, *26*, 2685–2694.
- Cengelli, F.; Maysinger, D.; Tschudi-Monnet, F.; Montet, X.; Corot, C.; Petri-Fink, A.; Hofmann, H.; Juillerat-Jeanneret, L. *J. Pharmacol. Exp. Ther.* **2006**, *318*, 108–116.
- Brigger, I.; Dubernet, C.; Couvreur, P. *Adv. Drug Delivery Rev.* **2002**, *54*, 631–651.
- Sun, S.; Zeng, H. *J. Am. Chem. Soc.* **2002**, *124*, 8204–8205.
- Shevchenko, E. V.; Talapin, D. V.; Kotov, N. A.; O'Brien, S.; Murray, C. B. *Nature* **2006**, *439*, 55–59.
- Hyeon, T.; Lee, S. S.; Park, J.; Chung, Y.; Na, H. B. *J. Am. Chem. Soc.* **2001**, *123*, 12798–12801.
- Casula, M. F.; Jun, Y. W.; Zaziski, D. J.; Chan, E. M.; Corrias, A.; Alivisatos, A. P. *J. Am. Chem. Soc.* **2006**, *128*, 1675–1682.
- Yu, W. W.; Chang, E.; Sayes, C. M.; Drezek, R.; Colvin, V. L. *Nanotechnology* **2006**, *17*, 4483–4487.
- Xie, J.; Peng, S.; Brower, N.; Pourmand, N.; Wang, S. X.; Sun, S. *Pure Appl. Chem.* **2006**, *78*, 1003–1014.
- Lin, C. L.; Lee, C. F.; Chiu, W. Y. *J. Colloid Interface Sci.* **2005**, *291*, 411–420.
- Ge, J.; Hu, Y.; Biasini, M.; Dong, C.; Guo, J.; Beyermann, W. P.; Yin, Y. *Chem.—Eur. J.* **2007**, *13*, 7153–7161.
- Ge, J.; Hu, Y.; Biasini, M.; Beyermann, W. P.; Yin, Y. *Angew. Chem., Int. Ed.* **2007**, *46*, 4342–4345.
- Hu, Y.; Ge, J.; Sun, Y.; Zhang, T.; Yin, Y. *Nano Lett.* **2007**, *7*, 1832–1836.
- Zhang, L.; He, R.; Gu, H. C. *Appl. Surf. Sci.* **2006**, *253*, 2611–2617.
- Chen, S. M.; Wu, G. Z.; Liu, Y. D.; Long, D. W. *Macromolecules* **2006**, *39*, 330–334.
- Mills, A.; LeHunte, S. *J. Photochem. Photobiol., A* **1997**, *108*, 1–35.
- Zhang, Q.; Gao, L.; Guo, J. *Appl. Catal., B* **2000**, *26*, 207–215.
- Joo, J.; Kwon, S. G.; Yu, T.; Cho, M.; Lee, J.; Yoon, J.; Hyeon, T. *J. Phys. Chem. B* **2005**, *109*, 15297–15302.
- Han, S. J.; Choi, S. H.; Kim, S. S.; Cho, M.; Jang, B.; Kim, D. Y.; Yoon, J.; Hyeon, T. *Small* **2005**, *1*, 812–816.
- Li, G.; Li, L.; Boerio-Goates, J.; Woodfield, B. F. *J. Am. Chem. Soc.* **2005**, *127*, 8659–8666.
- Trentler, T. J.; Denler, T. E.; Bertone, J. F.; Agrawal, A.; Colvin, V. L. *J. Am. Chem. Soc.* **1999**, *121*, 1613–1614.
- Jun, Y. W.; Casula, M. F.; Sim, J. H.; Kim, S. Y.; Cheon, J.; Alivisatos, A. P. *J. Am. Chem. Soc.* **2003**, *125*, 15981–15985.
- Cozzoli, P. D.; Kornowski, A.; Weller, H. *J. Am. Chem. Soc.* **2003**, *125*, 14539–14548.
- Kansal, S. K.; Singh, M.; Sud, D. *J. Hazard. Mater.* **2007**, *141*, 581–590.
- Anderson, C.; Bard, A. J. *J. Phys. Chem.* **1995**, *99*, 9882–9885.
- Jun, Y. W.; Choi, J. S.; Cheon, J. *Angew. Chem., Int. Ed.* **2006**, *45*, 3414–3439.
- Talapin, D. V.; Rogach, A. L.; Mekis, I.; Haubold, S.; Kornowski, A.; Haase, M.; Weller, H. *Colloids Surf. A* **2002**, *202*, 145–154.
- Bullen, C.; Mulvaney, P. *Langmuir* **2006**, *22*, 3007–3013.

NL071928T